

Adsorption of Anionic Dyes on Poly(N-vinylpyrrolidone) Modified Bentonite

D. Heddi^{a,b}, A. Benkhaled^b, A. Boussaid^a and E. Choukchou-Braham^{b,*}

^aLaboratoire de Recherche sur les Macromolécules (LRM), Université de Tlemcen, Algérie

^bLaboratoire de Recherche Toxicomed, Université de Tlemcen, Algérie

(Received 1 May 2019, Accepted 4 September 2019)

A composite, based on poly(N-vinylpyrrolidone) (PVP) and sodium bentonite, was prepared by a simple method. Structural characterizations of bentonite and the composite were performed by Fourier transform infrared spectroscopy (FTIR), X-ray diffraction (XRD) and thermogravimetric analysis (TGA). The TGA analysis showed a low loading of the polymer in bentonite. XRD analysis confirmed a modification in the structure of bentonite without affecting its crystalline nature. The prepared composite was used for the removal of Telon-blue, Telon-orange and Telon-red dyes in aqueous solution. Batch adsorption experiments were used to study the effect of the experimental parameters on the dyes equilibrium adsorption. At 23 °C, the maximum adsorption capacity obtained for the Telon-blue dye was 36.6 mg g⁻¹ (73.10%) after 120 min equilibrium time, 28.8 mg g⁻¹ (59.57%) after 40 min for orange-Telon, whereas, for Telon-red, we obtained 24.6 mg g⁻¹ (50%) after 60 min. The kinetic data of the adsorbed dyes were defined by the pseudo second order, and the equilibrium data were fitted well with the Freundlich isotherm. The thermodynamic parameters were determined for Telon-blue dye, as the more important adsorption capacity values were achieved for this dye. The adsorption process is non spontaneous and exothermic.

Keywords: Poly(N-vinylpyrrolidone), Bentonite, Composite, Telon, Adsorption

INTRODUCTION

Environmental pollution is an increasing concern in our societies. Regarding water pollution, it is urgent not only to stop rejections from industries and urbanisation, but also to remove the present pollution; for instance, the need of an efficient textile industry wastewater treatment is vital. The presence of dyes in effluents, even in low concentrations, is a major concern because they are highly visible, toxic, and contain microorganisms which are harmful to human health [1,2]. Azo dyes comprise a large group of dyes; they are natural or synthetic/organic compounds that can connect themselves to the surface or fabrics to provide a bright and lasting color [3]. Anionic dyes are colored compounds that are highly soluble in water and have reactive groups which are able to form covalent bonds between dye and fiber [4]; as a result, these dyes are the most widely used in the textile

Industry. However, the discharge of such effluents is of concern for both toxicological and environmental reasons. Various physical, chemical, and biological decolorization methods, such as adsorption, coagulation, membrane separation, electrochemical, dilution, filtration, flotation and reverse osmosis technologies, have been proposed [5-7]. Among them, adsorption is a simple and efficient process in terms of operation that can remove the contaminants even at very low concentrations.

Bentonite is a form of clay. It is the most commonly employed adsorbent for water treatment due to its high swelling capacity, large specific surface area and high cation exchange capacity. However, aggregation of the bentonite particles under varying conditions of temperature and electrolytes hamper its large scale application as an adsorbent. It is necessary to add certain additives or polymers to stabilize and prevent this adsorption process. Many papers have focused on the incorporation of polymers in the interlayer of clay minerals producing nanocomposites

*Corresponding author. E-mail: esma_sid@yahoo.fr

with adequate particle dispersion in water [8-10]. This simple modification of clay has been proposed to improve the adsorption properties of pollutants such as dyes [11,12] and heavy metals [13-15]. The use of polymer/bentonite as an adsorbent for the removal of dyes from water has been investigated in various studies, including polyacrylamide-bentonite [16], chitosan-bentonite [17] and polyvinylimidasole-bentonite [18]. Hence, the present study deals with the valorization of locally available bentonite clay from the fields of Maghnia (west Algeria) used as a biodegradable polymer-based composite poly(N-vinylpyrrolidone) as well as sodium bentonite as a new adsorbent used for the first time in the removal of anionic Telon dyes: blue, orange and red in aqueous solution. The effects of significant parameters such as contact time, pH, initial dyes concentration, temperature, composite dose and agitation speed on the adsorption efficiency of Telon dyes are evaluated. Also, thermodynamic, kinetic, and equilibrium parameters are investigated on the adsorption process.

EXPERIMENTAL

Adsorbent Material

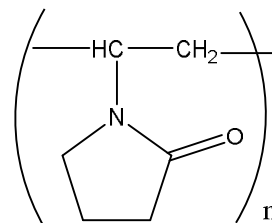
The non-ionic polymer, poly(N-vinylpyrrolidone) PVP (Scheme 1), with average molecular weight 58000 g mol^{-1} was provided from Sigma-Aldrich of Germany.

The natural clay sodium chloride-treated bentonite (sodium bentonite (Bt)) was provided from the fields of Maghnia, Algeria, National Company of Non-ferrous products (ENOF). The chemical composition of bentonite given by ENOF is shown in Table 1. The specific area of Bt was $79.83 \text{ m}^2 \text{ g}^{-1}$.

Dyes Solutions

Telon-dyes used in this study are organic anionic dyes industrially used for polyamide fibbers, namely Telon-blue ($\text{C}_{22}\text{H}_{14}\text{N}_6\text{O}_9\text{S}_2\text{Na}_2$) with a molecular weight 616.5 g mol^{-1} , Telon-orange ($\text{C}_{16}\text{H}_{11}\text{N}_2\text{NaO}_4\text{S}$) with a molecular weight $350.32 \text{ g mol}^{-1}$ and Telon-red ($\text{C}_{22}\text{H}_{16}\text{N}_3\text{NaO}_6\text{S}_2$) with a molecular weight 505.5 g mol^{-1} .

The stock solutions of the dyes were prepared by dissolving a quantity of the dye in distilled water. All working solutions were obtained by successive dilutions. At



Scheme 1. Molecular Structure of PVP

various times, the concentration of dyes remaining in the solution after adsorbent contact and centrifugation of the composite was determined using a UV-Vis spectrophotometer at the maximal adsorption wavelength (λ_{max} , 498 nm for red, 609 nm for blue and 490 nm for orange Telon).

Preparation of the Adsorbent

The composite PVP/Bt was prepared according to the procedure described in previous papers [15,19]. A concentration of 100 g l^{-1} of Bt (1 g) was used for preparation of the composite samples. A magnetic stirrer was used for 24 h to disperse Bt in water at room temperature. Then, the PVP polymer (0.18 g), with a concentration of 60 g l^{-1} dissolved in water was added drop wise to the Bt suspension. The mixture was stirred at room temperature for 24 h, then centrifuged at 3000 rpm for 20 min. In order to obtain the final product, the sediment was washed with distilled water five times and dried at $60 \text{ }^\circ\text{C}$ for one day.

Characterization

Sodium bentonite, PVP and the composite were characterized using a Fourier transform infrared spectrometer (FTIR) Agilent Technologies Cary 600 Series (USA) to confirm the formation of the composite and the interaction between the polymer and the bentonite. An X-Ray Diffractometer Rigaku Americas Ultima IV with a Cu K_α radiation of 1.54 \AA was used to project the formation of the intercalated composite and characterize the presence of impurities in the range of 2 theta (2θ) from 3° - 15° with a step of 0.02° . Thermogravimetric analysis (TGA) was used to study the thermal stability of the composite and to determine the weight loss at each temperature.

Table 1. Chemical Composition of Bentonite

Chemical composition	SiO ₂	Al ₂ O ₃	Fe ₂ O ₃	MgO	K ₂ O	CaO	TiO ₂	Na ₂ O	As	Loss on ignition
Wt. %	64.7	18.1	0.95	2.66	0.8	0.61	0.2	1.43	0.05	10.0

Thermogravimetric analysis was carried out on a TGA Q50V6.7. Build 203 instruments, Germany, with a heat rate of 10 °C min⁻¹ from 20 °C to 800 °C. For the dyes concentration determination, UV-Vis spectrophotometer analytic SPECORD 200 plus, Germany, was used.

Adsorption Experiments

Dyes adsorption was investigated at 23 °C. The kinetic study was carried out using 1 g l⁻¹ of adsorbent dose with an initial concentration of dyes of 0.05 g l⁻¹. The experiments were realized in flasks shaken on a horizontal shaker at the constant vibration rate of 450 rpm. After adsorption, the solution was centrifuged at 3000 rpm for 10 min and an aliquot of the supernatant was analyzed by UV-Vis spectroscopy. All measurements were recorded at the wavelength corresponding to maximum absorbance, λ_{max} , for each dye.

The pH of the solutions was maintained at the required pH value by adding appropriate amounts of 0.1 M NaOH or HCl. The mixtures were then stirred at 23 °C and the amounts of adsorbed dyes remaining in the supernatant solutions were identified spectrophotometrically. The studies of adsorption isotherms were performed using 1 g l⁻¹ of adsorbent dose at various concentrations ranging from 0.01-0.1 g l⁻¹. The effect of temperature on the adsorption capacity was also studied as variable from 25 °C to 55 °C. The effect of adsorbent dose was studied over the range of 0.2-4 g l⁻¹ while the concentration of dyes maintained constant (0.05 g l⁻¹).

The adsorption capacity of dyes adsorbed on the composite (q_e , mg g⁻¹) was calculated as follows (Eq. (1)): [20]

$$q_0 = (C_i - C_0) \times \frac{V}{m} \quad (1)$$

Similarly, the adsorption efficiency (%) of dyes on the

composite was calculated by the following equation (Eq. (2)) [20]:

$$Adsorption (\%) = \frac{C_i - C_0}{C_i} \times 100 \quad (2)$$

where C_i (mg l⁻¹) is the initial dyes concentration, C_0 (mg l⁻¹) is the equilibrium concentration of dyes in the supernatant after centrifugation, V (l) is the volume of the dye solution and m (g) is the adsorbent mass.

RESULTS AND DISCUSSION

Characterization of the Adsorbent

FTIR analysis. The chemical structure of Bt and the composite were analyzed by FTIR spectrometry. The obtained spectra of bentonite and PVP are shown in Fig. 1, curves a) and b), respectively. The band located in the range 3620-3680 cm⁻¹ corresponds to the stretching vibrations of the OH groups of the octahedral layer and the deformation vibrations of the H₂O molecules. The small peak (curve a) observed at around 1634 cm⁻¹ is attributed to the deformation of HO-H of water. The strong band at 1000 cm⁻¹ represents the characteristic vibrations band of Si-O [21]. For PVP (Fig. 1, curve b), the peaks monitored at 3478 cm⁻¹ are assigned to O-H stretching, and the peaks at 1423 cm⁻¹ and 845 cm⁻¹ corresponding to the CH₂ scissoring vibrations and CH₂ bending, respectively. The peaks at 1642 cm⁻¹ and 1277 cm⁻¹ are apportioned to C=O stretching and C-N stretching [22]. The spectrum of the composite in Fig. 1, curve c shows the presence of the typical bands of bentonite and only an intensity decrease for the bands at 1000 cm⁻¹ corresponding to the Si-O band and 917 cm⁻¹ of Al-O compared to the similar bands in bentonite (Fig. 1, curve a). The interaction between PVP and Bt occurred by the formation of hydrogen bonds between the C=O groups

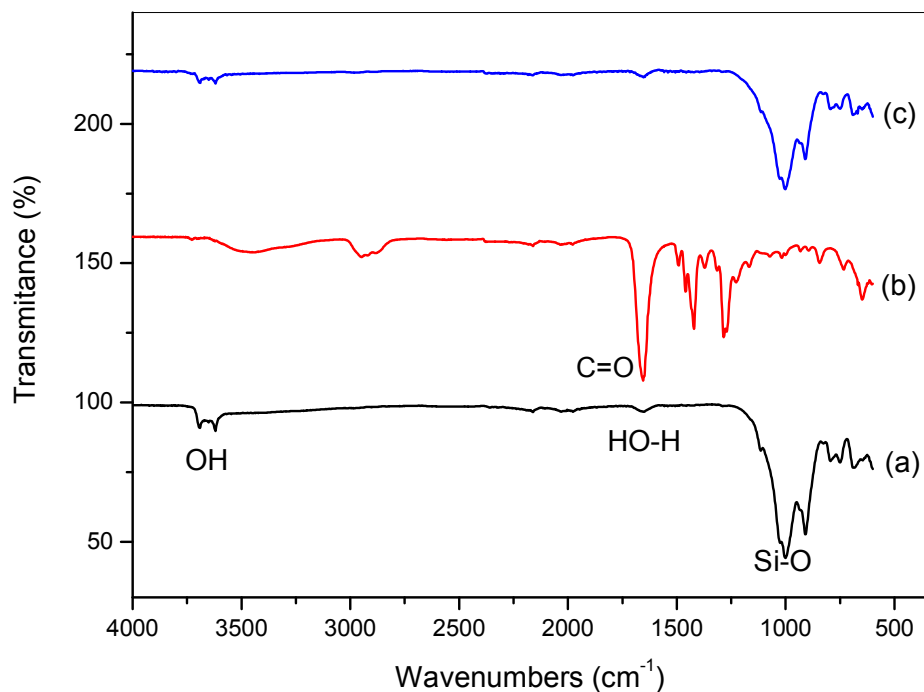


Fig. 1. FTIR spectra of Bt (curve a), PVP (curve b) and PVP/Bt (curve c).

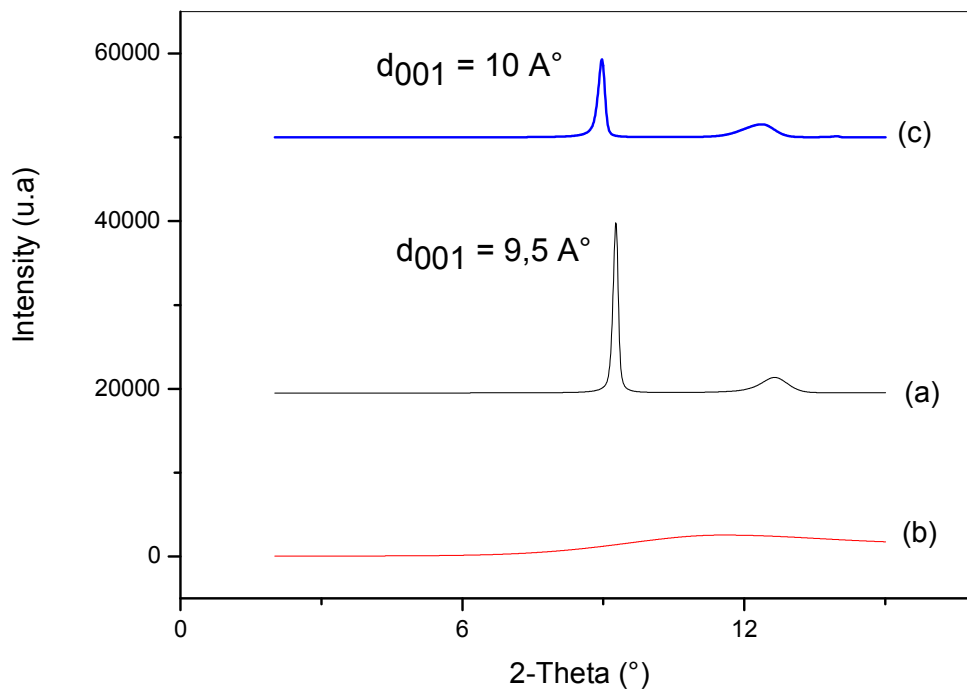


Fig. 2. Diffractograms of Bt (curve a), PVP (curve b) and PVP/Bt (curve c).

of PVP and the OH groups of silanol on the surface of the sodium bentonite, as described elsewhere [23].

On the other hand, the band of C=O in the composite was not identified. Indeed, the IR spectrum of the composite does not show clearly the introduction of PVP into the sodium bentonite, so, another method of characterization, such as the XRD, was needed.

XRD Analysis

XRD is an available technique most commonly used to probe the clay modification by changes in the position, shape and intensity of the peak due to the (001) basal spacing of the crystalline structure of the clay; it can be used to verify the modification of the bentonite layers spacing due to the intercalation of organic polymers. Furthermore, the disappearance of this peak indicates the exfoliation of the bentonite layers [24]. X-ray diffraction studies were conducted on Bt, PVP and PVP/Bt. The X-ray powder profile of PVP (Fig. 2, curve b) showed the polymer is amorphous whereas the diffractogram of Bt confirmed the presence of montmorillonite peaks at $2\theta = 9.2^\circ$ with $d_{001} = 9.5 \text{ \AA}$.

On the other part, the X-ray diffraction pattern of the composite (Fig. 2, curve c) showed an increase in interlayer spacing d_{001} from 9.5 \AA to 10 \AA compared with Bt, as well as a shift of the diffraction peak towards lower angle values from $2\theta = 9.2^\circ$ (Bt) to $2\theta = 8.9^\circ$ for PVP/Bt. We suggest that the composite 001 peak shift to the lower angles is due to the insertion of a few polymer chains into the interlayer spaces of Bt, increasing slightly the average spacing. This result indicates that the PVP might lie flat on the silicate surface as a monolayer and with a vertical orientation comparable to other organo-clay systems cited by B. Makhoukhi *et al.* [25]

TGA Analysis

Thermogravimetry is an essential method for studying the thermal stability of polymers; in our study we have used the TGA analysis for the determination of PVP intercalation in bentonite. TGA thermograms of Bt, PVP and PVP/Bt are illustrated in Fig. 3. For Bt (Fig. 3, curve a), a 0.5 % weight-loss was recorded in the temperature range of 0-100 °C, corresponding to the evaporation of the physically adsorbed water molecules trapped in the bentonite interlayers. A

4.5% weight-loss in the temperature range of 380-600 °C is related to the removal of water molecules from the crystal lattice, with one alumina octahedral sheet sandwiched between two silica tetrahedral sheets. The presence of carbon and Cl is attributed to degradation of organic impurity molecules and to NaCl traces, respectively, in bentonite [26]. The thermogram of PVP (Fig. 3, curve b) shows 10% weight loss between 0 and 100 °C due to water molecules adsorbed by this hygroscopic polymer. The largest weight loss (80%), ranging from 380-600 °C, is related to the thermal decomposition of PVP.

For the composite thermogram represented in curve c of Fig. 3, 2.3% weight loss was recorded at the temperature range of 0-200 °C and 7.8% weight loss appeared at 380-800 °C. The first is due to the evaporation of adsorbed water, the second is related to the decomposition of the PVP polymer. The amount of the composite weight loss between 380 and 600 °C (7.8%) was larger than that of Bt (4.5%) so the amount of the intercalated polymer deduced from TGA was estimated to be 3.3. Thus, the bentonite modified with PVP increased the thermal stability of the composite [15].

Zeta Potential

The values of the zeta potentials of Bt and PVP/Bt are -0.420 mV and -0.216 mV, respectively. These results indicate that the negative charge on the PVP/Bt composite was reduced compared to that of Bt. This reduction of negative charges can be explained by the screen of Bt negative charges by the polymer confirming the insertion of PVP on the silicate surface of sodium bentonite.

Adsorption Studies

Effect of contact time. Before starting the kinetic study of dyes; a retention test was performed on the bentonite and the composite to get an idea about the best adsorbent of the three dyes.

Figure 4 shows the adsorption percentages for each anionic dye by Bt and PVP/Bt. The results show an improvement of the adsorption efficiency of dyes on the composite compared to the sodium bentonite from 45.23% to 73.1% for Telon-blue, from 41.2% to 59.57% for Telon-orange and from 36.8% to 50% for Telon-red. The adsorption efficiency for Telon-blue is better than Telon-orange and Telon-red.

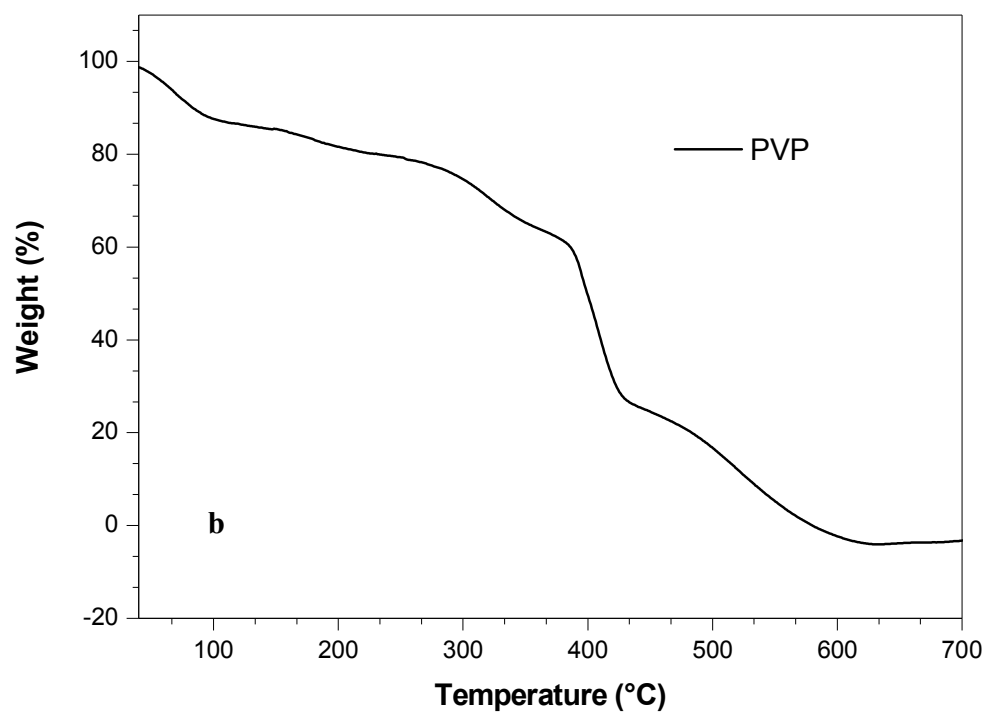
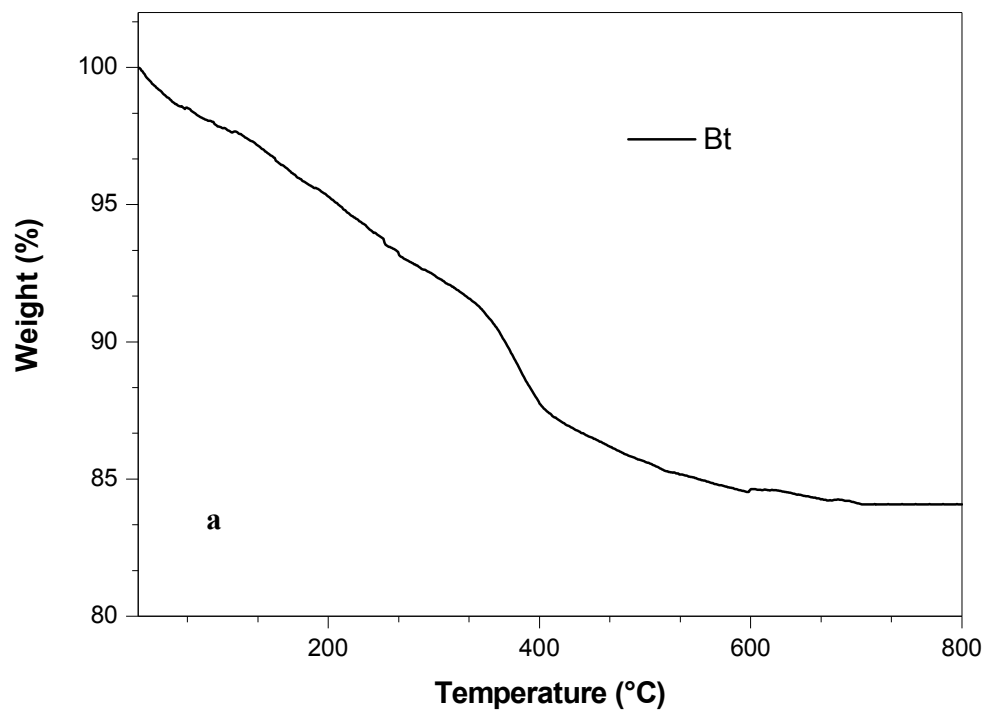


Fig. 3. TGA of a) Bt, b) PVP and c) PVP/Bt.

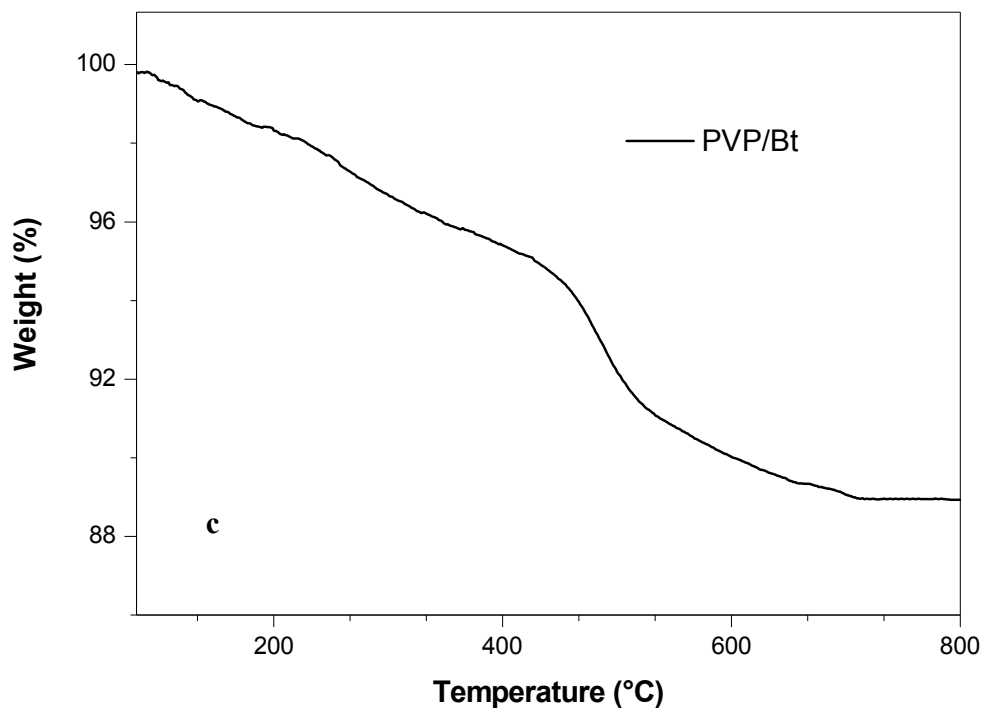


Fig. 3. Continued.

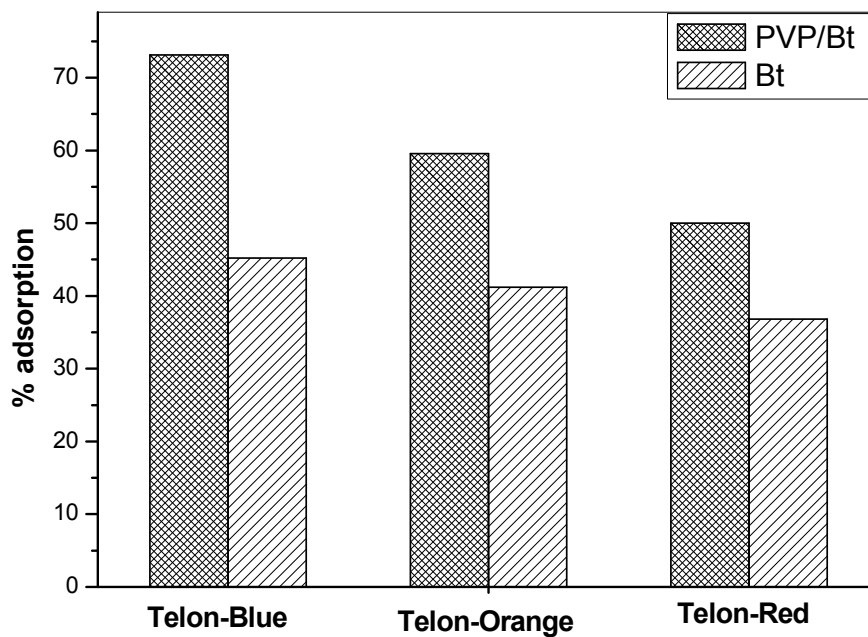


Fig. 4. Dyes removal percentage on sodium bentonite and composite (Conditions: adsorbent dose 1 g l^{-1} , pH 6.15, initial dyes concentration 0.05 g l^{-1} , temperature $23 \text{ }^\circ\text{C}$, contact time 240 min, and agitation speed 450 rpm).

Figure 5 shows the influence of contact time on the dyes in their aqueous solutions with the PVP/Bt composite. The dyes removal was rapid in the initial stages of contact time, then increased slowly with further contact time and remained constant when the equilibrium time was reached. The equilibrium position was attained after 40 min for Telon-orange, 60 min for Telon-red and after 120 min for Telon-blue.

The adsorption capacity for Telon-blue was 36.6 mg g^{-1} with an adsorption efficiency of 73.1%, whereas the adsorption capacity of Telon-orange and Telon-red was 28.8 mg g^{-1} , and 24.6 mg g^{-1} , with an adsorption efficiency of 59.6% and 50%, respectively.

Adsorption Kinetics Model

In order to investigate the process involved in the adsorption of the dyes onto the composite, pseudo-first-order and pseudo second-order kinetic models were used. These models are defined, respectively by Eqs. (3) and (4) [27]:

$$\ln(q_e - q_t) = \ln q_e - k_1 t \quad (3)$$

$$\frac{t}{q_t} = \frac{1}{k_2 q_e^2} + \frac{1}{q_e} t \quad (4)$$

Here, q_e and q_t are the adsorption capacities (mg g^{-1}) at equilibrium and after contact time t (min) of adsorption, respectively. k_1 (min^{-1}) and k_2 (min g mg^{-1}) are the pseudo-first and pseudo-second-order rate constants, respectively.

The adsorption rate constant for the first-order kinetics can be determined from the plot of $\ln(q_e - q_t)$ against t . The equilibrium adsorption capacity (q_e) and the second-order rate constant k_2 can be determined experimentally from the slope and intercept of the plot of t/q_t vs. t . The kinetic parameters for the pseudo-first and pseudo-second order kinetic models, based on Eqs. (3) and (4), are shown in Table 2.

The kinetic data for the dyes were best fitted to the pseudo-second order model, as shown by the highest correlation coefficients ($R^2 = 0.99$ for the three Telon dyes) in relation to the linear variation of t/q_t with time t , as shown in Fig. 6. The calculated amounts of dyes adsorbed at equilibrium (q_e) were very close to the experimentally

obtained values (Table 2). The rate constants of the pseudo-second-order model were for Telon-blue $0.010 \text{ min g mg}^{-1}$, faster than the $1.78 \times 10^{-4} \text{ min g mg}^{-1}$ and $0.36 \times 10^{-4} \text{ min g mg}^{-1}$ for Telon-red and Telon-orange, respectively.

Effect of the Solution pH

The pH value of the dye solutions, affecting the surface charge of the adsorbent, is an important controlling parameter in the adsorption process [28]. Consequently, the investigation of the effect of pH on the adsorption process was helpful to reveal the adsorption mechanism. The effect of pH on the adsorption of dyes from 0.05 g l^{-1} concentrations by the composite was studied by varying the pH from 3 to 11.8, as shown in Fig. 7. The adsorption efficiency of all three dyes increased from pH 3 to pH 6.15, then decreased when the pH value exceeded 6.15 (Fig. 7). The high adsorption of anionic dyes was due to the protonated form of composite PVP/Bt-OH₂⁺ and the electrostatic attraction occurred between the protonated sites and the anionic groups (-SO₃⁻) of the dyes, causing an increase of the dye adsorption.

The same results were observed by Makhoukhi *et al.* [29] when they used diphosphonium ion-exchanged montmorillonite for the adsorption of the same anionic dyes; better adsorption was obtained in an acidic medium. Another adsorbent such as poly (N-octyl-4-vinylpyridinium bromide) used by our group previously [30] for Telon-orange dye adsorption also gave the same result.

However, with an increase in pH, the protonated form of the composite disappeared and the composite existed in the form of PVP/Bt-OH⁻ so lower adsorption efficiency was observed. In the case of an abundance of hydroxide (OH⁻) ions, a repulsion between the anionic dyes and the negatively charged sites of the composite occurred.

We can also notice that the adsorption capacity of the Telon-blue dye increased than the other two dyes from pH 3 to pH 6.15. This dye, containing two anionic sites, appears to be more reactive than the other two dyes with a single anionic site.

Adsorption Isotherms

The Langmuir and Freundlich models are commonly used to describe the removal of pollutants from water and

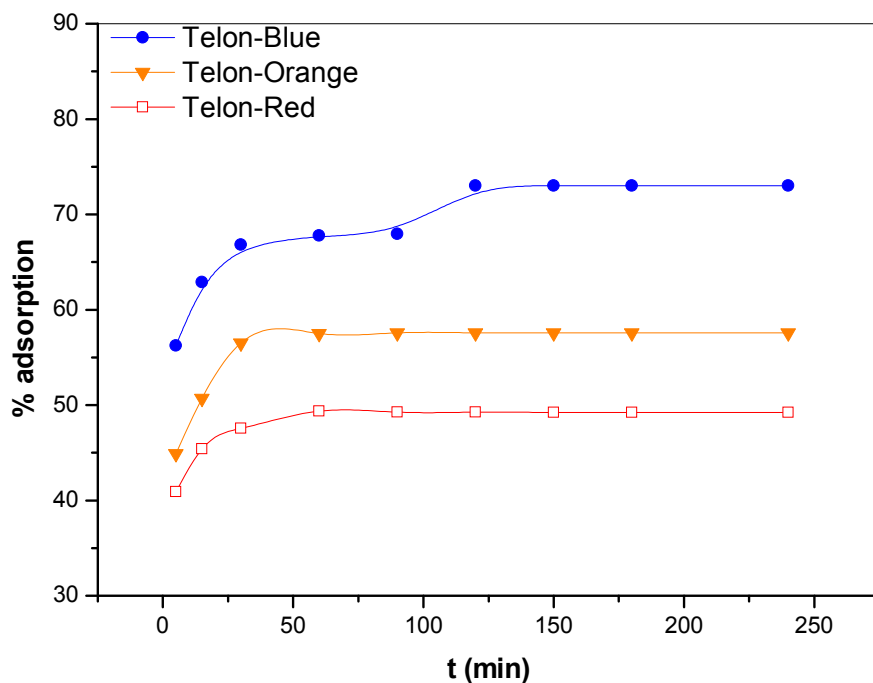


Fig. 5. Effect of contact time on removal of anionic dyes by PVP/Bt composite; (Conditions: adsorbent dose 1 g l^{-1} , pH 6.15, initial dyes concentration 0.05 g l^{-1} , temperature $23 \text{ }^\circ\text{C}$, and agitation speed 450 rpm).

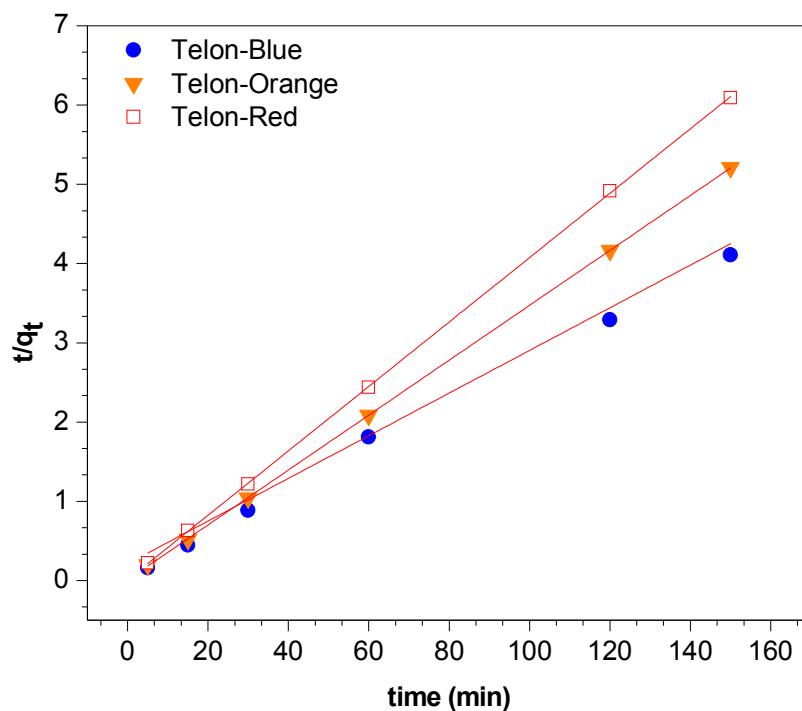


Fig. 6. Kinetic plots of the pseudo-second order model for the adsorption of dyes on PVP/Bt composite under the experimental conditions.

Table 2. Kinetic Parameters for Dyes Adsorption on PVP/Bt

	Pseudo-first order				Pseudo-second order		
	q_e exp.	k_1	q_e calc.	R^2	k_2	q_e calc.	R^2
	(mg g^{-1})	(min^{-1})	(mg g^{-1})		(min g mg^{-1})	(mg g^{-1})	
Telon-blue	36.50	0.01	4.41	0.80	0.01	36.40	0.99
Telon-orange	28.78	0.02	1.06	0.72	$3.56 \cdot 10^{-5}$	24.61	0.99
Telon-red	24.62	0.07	0.42	0.37	$1.78 \cdot 10^{-4}$	29.05	0.99

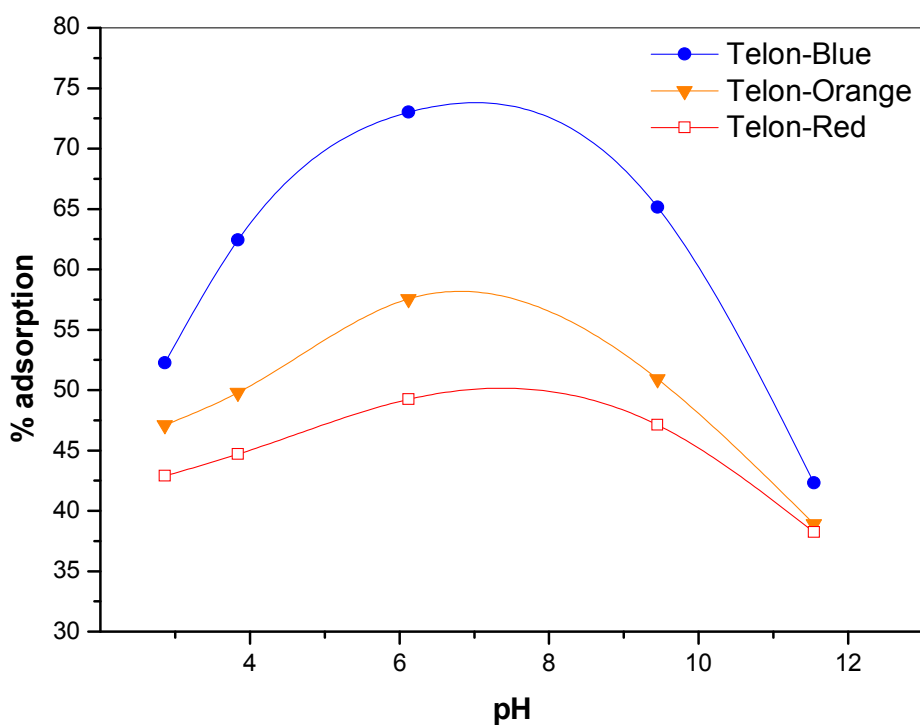


Fig. 7. Effect of pH on the adsorption of anionic Telon dyes on PVP/Bt composite (Conditions: adsorbent dose 1 g l^{-1} , initial dyes concentration 0.05 g l^{-1} , temperature $23 \text{ }^\circ\text{C}$, contact time 240 min, and agitation speed 450 rpm).

effluents.

Langmuir model is based on the assumption that the adsorption occurs on homogeneous surfaces. The Langmuir form isotherm model can be written as following [31,32]:

$$\frac{C_e}{q_e} = \frac{1}{K_L q_m} + \frac{C_e}{q_m} \tag{5}$$

where K_L and q_m are the constants of Langmuir isotherm

model indicating the adsorption energy ($l \text{ g}^{-1}$) and the maximum adsorption capacity (mg g^{-1}), respectively.

Freundlich isotherm describes adsorption process where the adsorbent has heterogeneous surfaces with different energies. Equation (2) presents the linearized form of this equation [31,32]:

$$\ln q_e = \ln K_F + \frac{1}{n} \ln C_e \quad (6)$$

where K_F and n are the model constants showing the relationship between adsorption capacity and adsorption intensity, respectively. $n = 1$ shows that the adsorption process is linear, $n < 1$ indicates chemical adsorption process, and $n > 1$ shows that the adsorption is a physical process [31,32]. The constants of K_F and n are determined from the intercept and slope of the plot of $\ln q_e$ against $\ln C_e$.

Figure 8 presents the equilibrium isotherms for the dye adsorptions onto the composite. It is evident that the equilibrium adsorption capacity (q_e) increased with the equilibrium dyes concentration (C_e). The shape and initial slope of the Telon dyes adsorption isotherm belong to the L-type isotherm of the Giles classifications [33]. L-type isotherms are usually associated with ionic solute adsorption with weak competition with the solvent molecules.

The fitting of the Langmuir and Freundlich models to the experimental dyes removal data are shown in Figs. 9a and b, respectively. The parameters for the linear Freundlich and Langmuir isotherms are shown in Table 3. Better linearity was observed using the Freundlich model for all isotherms in the whole range of concentration investigated, with the correlation coefficients 0.99 for the three dyes. The better linearity of Freundlich was apparently due to heterogeneities of the composite surface and to the dyes adsorbent interactions with the composite. The latter may also depend strongly on the chemical structure of the dyes molecules. The values of n for the adsorption of blue, orange and red Telon dyes were about 1.66, 1.36 and 1.28, respectively, indicating that the process was physisorption. In conclusion, the appropriate model for the three dyes was the Freundlich model. The same result was also found onto diphosphonium ion-exchanged montmorillonite [29].

The maximum amounts of adsorption of Telon-blue, Telon-orange and Telon-red were determined by the

Langmuir model, but they were found inadequate with experimental ones which are 59.56 mg g^{-1} , 39.08 mg g^{-1} and 35.42 mg g^{-1} , for blue, orange and red, respectively.

Makhoukhi *et al.* determined the maximum adsorption capacities of three Telon dyes using bis-imidazolium modified bentonite diphosphonium (organo-Bt) [34] and diphosphonium ion-exchanged montmorillonite: *para*, *meta* and *ortho* (triphenyl phosphonium methylene)-benzene-dichloride (*p*-, *m*- and *o*-TPhPMB) [29], a comparison on the maximum adsorption capacity obtained with these adsorbents and our composite PVP/Bt is shown in Table 4. We deduce that the maximum adsorption capacity of Telon-blue using the composite PVP/Bt presented in this study is larger than that in previous works.

Thermodynamic Parameters

The effect of temperature on adsorbent dosage and stirring speed were studied for the Telon-blue dye which had the better adsorption on our composite compared with Telon-orange and Telon-red.

The temperature is a parameter known to affect the transport/kinetic processes of dye adsorption. Therefore, the thermodynamic activation parameters of the process, of the dye adsorption process onto the composite PVP/Bt, were determined using Eqs. (7) and (8) [35,36]:

$$\Delta G^\circ = -RT \ln K_c \quad (7)$$

$$\Delta G^\circ = \Delta H^\circ - T\Delta S^\circ \quad (8)$$

where T is the temperature in Kelvin, R is the ideal gas constant ($8.314 \text{ J mol}^{-1} \text{ K}^{-1}$), ΔH° is the enthalpy, ΔS° the entropy, ΔG° is the free energy, and K_c is the equilibrium constant equivalent to the fractional amount of the dye adsorbed onto the composite; it is calculated from [35,36]:

$$K_c = \frac{q_e}{C_e} \quad (9)$$

q_e and C_e are the capacity of adsorption and the equilibrium concentration of dye (mg l^{-1}) in the solution.

The values of ΔS° and ΔH° can be calculated from the intercept and slope of the $\ln K_c$ vs. $1/T$ plot, expressed in Eq. (10).

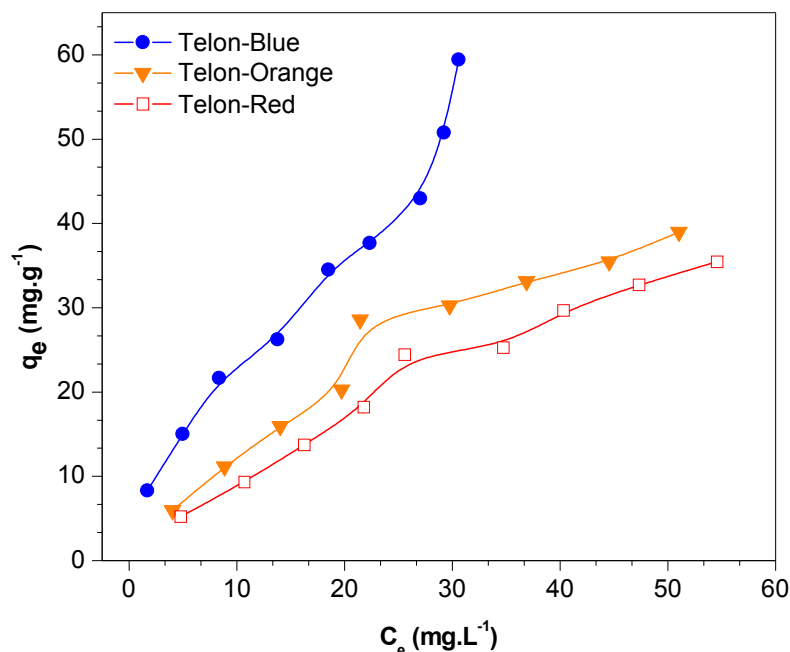


Fig. 8. Isotherm plots (q_e vs. C_e) for adsorption of dyes on PVP/Bt (Conditions: adsorbent dose 1 g l^{-1} , pH 6.15, temperature $23 \text{ }^\circ\text{C}$, contact time 240 min, and agitation speed 450 rpm).

Table 3. The Parameters for Freundlich and Langmuir Adsorption of Dyes on PVP/Bt

	Freundlich coefficients			Langmuir coefficients		
	n	K_F	R^2	q_m (mg g^{-1})	K_L (l mg^{-1})	R^2
Telon-blue	1.66	6.03	0.99	53.87	0.10	0.94
Telon-orange	1.36	2.27	0.99	72.72	0.03	0.98
Telon-red	1.28	1.54	0.99	70.27	0.03	0.98

$$\ln K_c = \frac{\Delta S^\circ}{R} - \frac{\Delta H^\circ}{RT} \quad (10)$$

Figure 10 shows the adsorption efficiency of the Telon-blue dye onto PVP/Bt as a function of the temperature. It is noteworthy that the adsorption efficiency decreases with increasing temperature indicating a reduction in the spontaneous degree of the process and a driving force leading to decrease in the adsorption capacity [37,38].

The parameters of the linear fit $\ln K_c$ vs. $1/T$ (Fig. 11) are presented in Table 5. The ΔH° value was negative, indicating the exothermic nature of the adsorption process of the Telon-blue dye. Moreover, the negative values of ΔS° indicate that the randomness decreased at the solid-liquid interface during the adsorption process. In addition, the positive ΔG° values of the adsorption indicated that the Telon-blue adsorption process is non spontaneous.

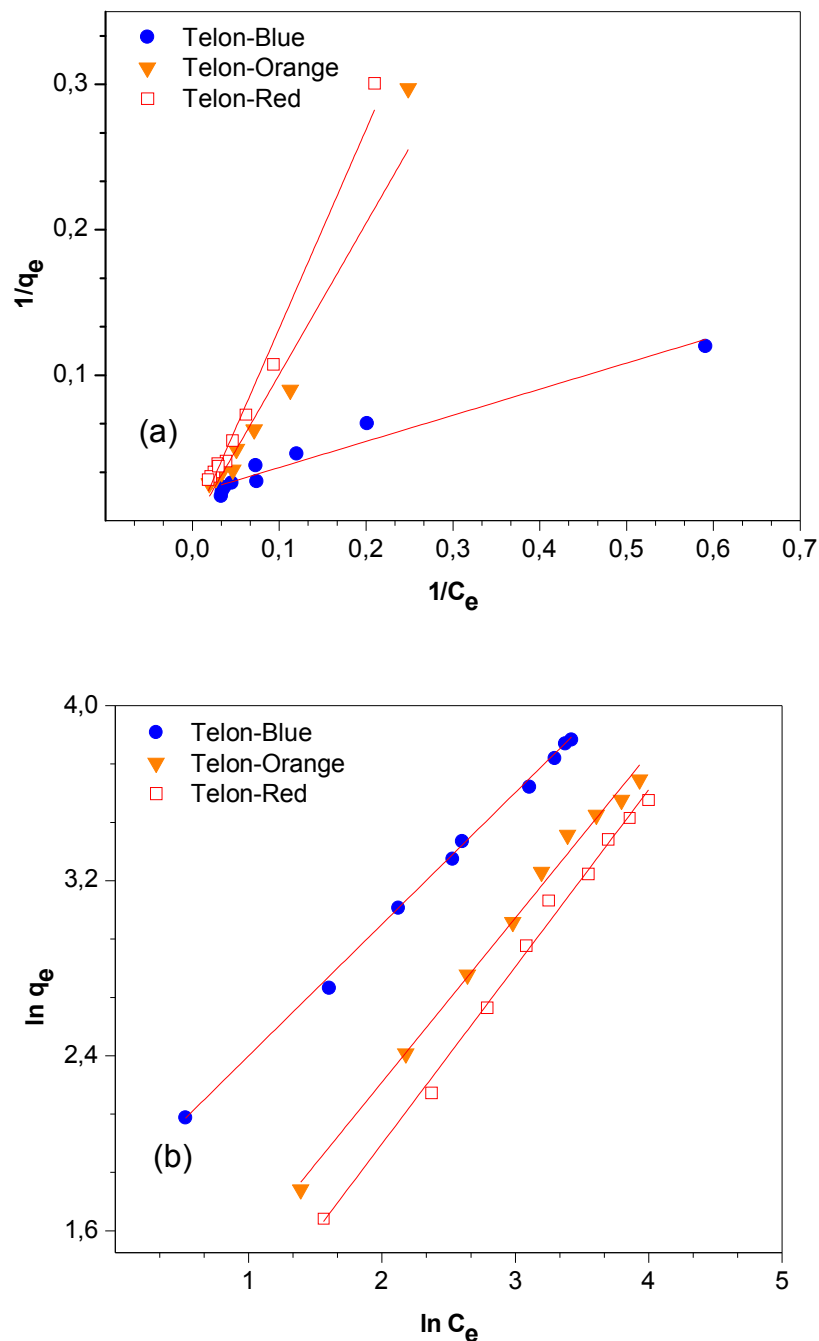


Fig. 9. Adsorption isotherms of Telon dyes on PVP/Bt: a) Langmuir, and (b) Freundlich.

Effect of Adsorbent Dosage

In order to determine the influence of adsorbent dosage on the dyes adsorption, experiments were carried out with an initial concentration of 0.05 g l^{-1} for Telon-blue, while

the adsorbent dose was varied from 0.2 g l^{-1} to 4 g l^{-1} . As shown in Fig. 12, the adsorption efficiency increases from 42.74% up to 86.40% with increasing the adsorbent dose.

This can be due to the increase and availability of

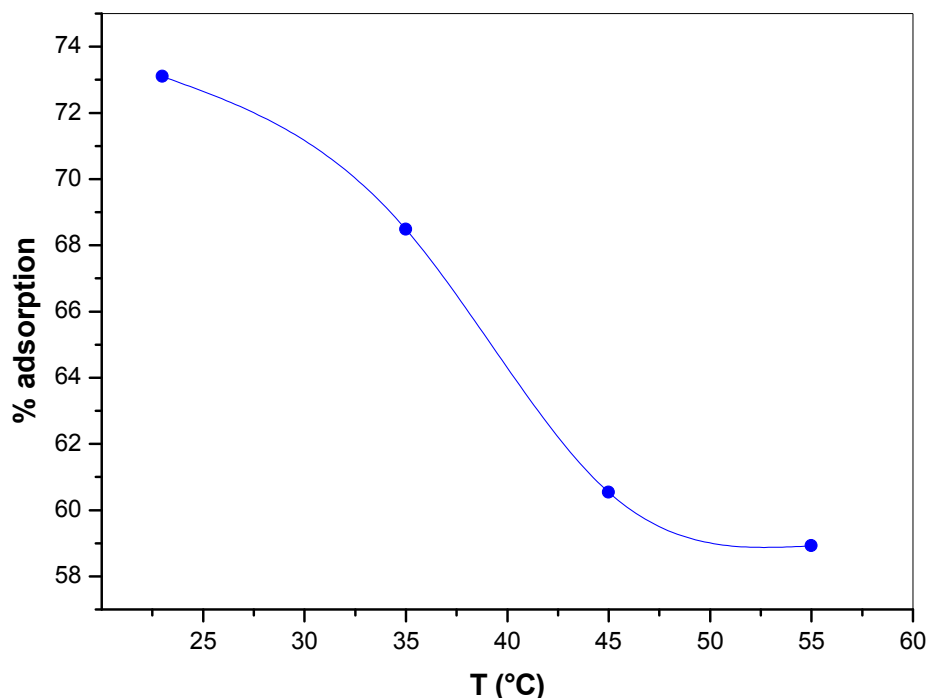


Fig. 10. Influence of temperature on adsorption of Telon-blue dye on PVP/Bt. $C_{\text{dye}} = 0.05 \text{ g l}^{-1}$, $m_{\text{adsorbent}} = 1 \text{ g}$, $V_{\text{solution}} = 1 \text{ l}$, $\text{pH}_{\text{dye}} = 6.15$. (Conditions: adsorbent dose 1 g l^{-1} , pH 6.15, initial dyes concentration 0.05 g l^{-1} , contact time 240 min and agitation speed 450 rpm).

Table 4. The Maximum Adsorption Capacity Obtained for Telon Dyes by Adsorbents

	C_i (mg l^{-1})	<i>p</i> -TPhPMB-		<i>m</i> -TPhPMB-		<i>o</i> -TPhPMB-	
		PVP/Bt q_{max} (mg g^{-1})	Mt q_{max} (mg g^{-1})	Mt q_{max} (mg g^{-1})	Mt q_{max} (mg g^{-1})	Organo-Bt q_{max} (mg g^{-1})	
Telon-blue	100	59.56	30	28	21	58	
Telon-orange	100	39.08	58	40	38	76	
Telon-red	100	35.42	29	22	22	68	

adsorption active sites and enough surfaces of adsorbent by increasing its dosage [27]. Besides, a rise in utilization of adsorbent dosage is accompanied by a decrease of the adsorption capacity from 107 mg g^{-1} to 2.44 mg g^{-1} which is attributed to unsaturation of a large number of active

sites during the adsorption process [27]. The same results were observed in our previous work [30] using the copolymer poly (N-octyl-4-vinylpyridinium bromide) for the adsorption of Telon-orange.

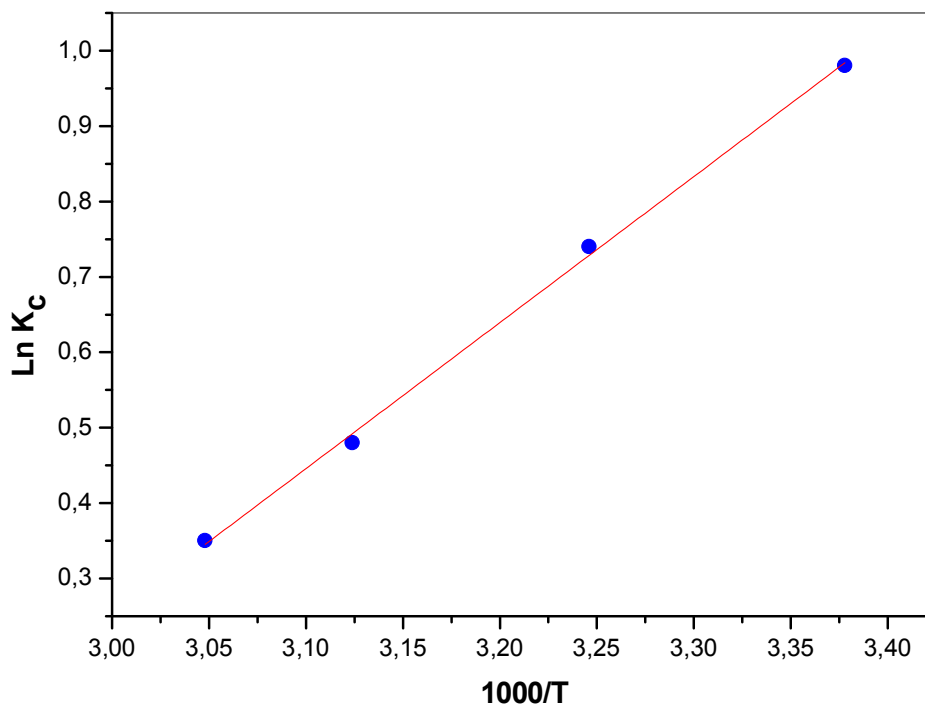


Fig. 11. The Van't Hoff plot for the adsorption of Telon-blue dye on PVP/Bt.

Table 5. Thermodynamic Parameters of the Telon-blue Adsorption on PVP/Bt at Various Temperatures

	ΔH° (J mol ⁻¹)	ΔS° (J mol ⁻¹ K ⁻¹)	R ²	ΔG° (kJ mol ⁻¹) 296 K	ΔG° (kJ mol ⁻¹) 308 K	ΔG° (kJ mol ⁻¹) 318 K	ΔG° (kJ mol ⁻¹) 328 K
Telon-blue	-16.04	-46.14	0.99	47.01	48.94	50.54	52.14

Effect of Stirring Speed

The stirring rate plays an important role in the transfer of the solute molecules to the adsorbent. It is therefore interesting to study this parameter. Figure 13 shows the variation of the adsorption capacity and the adsorption efficiency of adsorbed Telon-blue on the PVP/Bt composite as a function of the stirring speed.

Note that, the adsorption efficiency increased slightly as the stirring rate increased. It is clear that adsorption efficiency of Telon-blue at equilibrium was almost independent of the stirring speed in the range studied

indicating that the dye had equivalent access to adsorbent at all the stirring speeds used. The experiment shows that the stirring speed has no significant influence on the dye adsorption in the studied range between 150 and 750 rpm.

CONCLUSIONS

The retention of anionic Telon dyes by sodium bentonite and composite poly (N-vinylpyrrolidone) modified sodium bentonite was studied here. The results obtained show a marked improvement in the retention of three Telon dyes

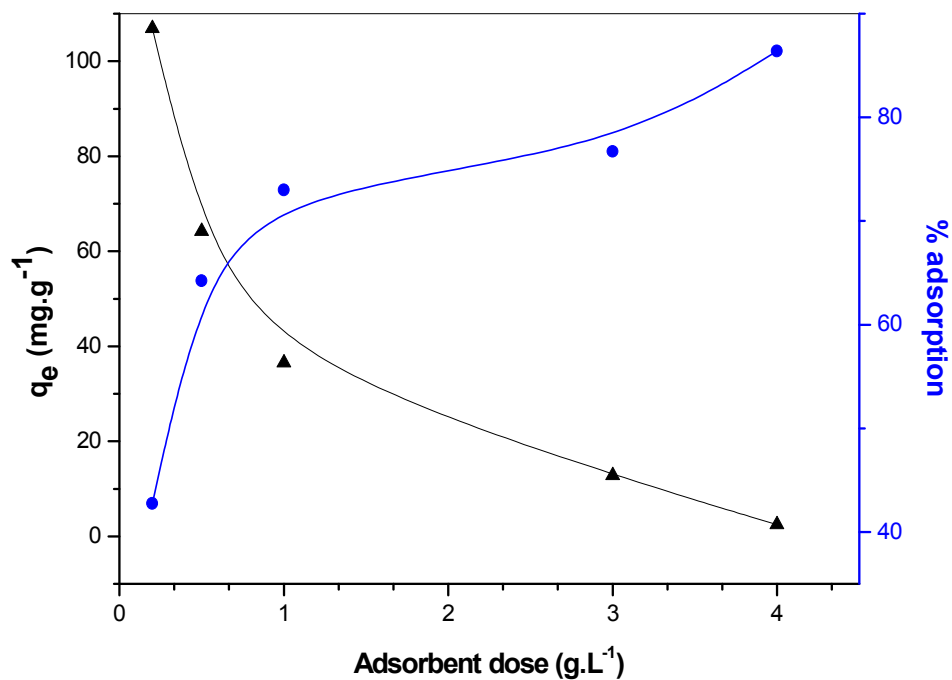


Fig. 12. Effect of adsorbent weight on adsorption capacity of Telon-blue (Conditions: pH 6.15, initial dyes concentration 0.05 g l⁻¹, temperature 23 °C, contact time 240 min, and agitation speed 450 rpm).

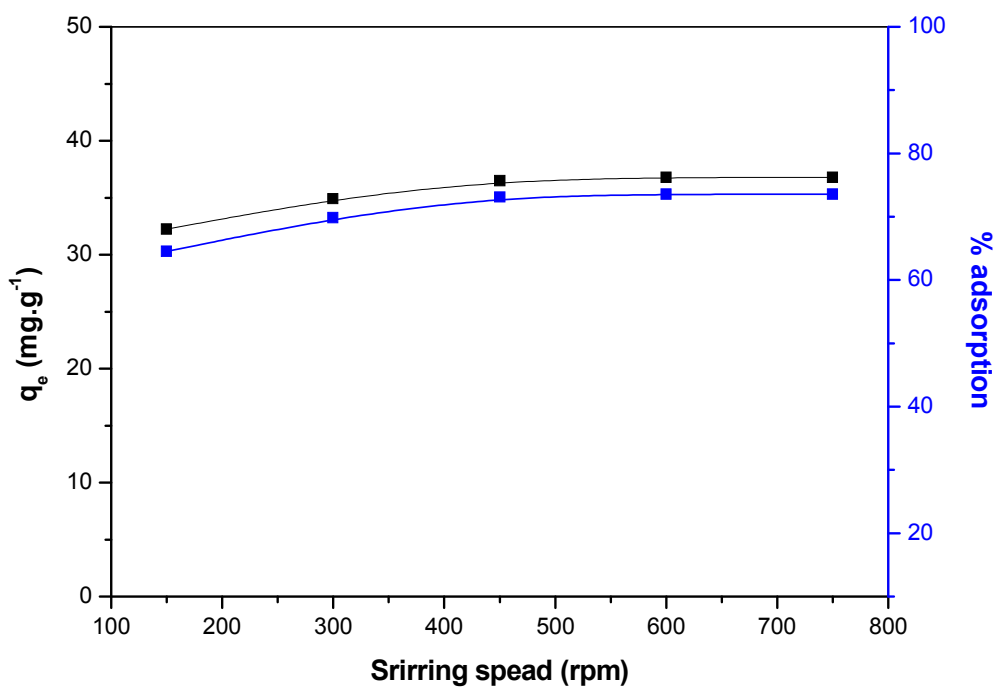


Fig. 13. Effect of the stirring speed on the Telon-blue adsorption capacity (Conditions: adsorbent dose 1 g l⁻¹, pH 6.15, initial dyes concentration 0.05 g l⁻¹, temperature 23 °C, and contact time 240 min).

using PVP inserted in sodium bentonite at the same experimental condition. This research provided evidence on intercalation of PVP in the interlayer of sodium bentonite of Maghnia. Indeed, the effect of various parameters on the adsorption efficiency was studied and the results showed that dye adsorption capacity increased by increasing initial concentration and contact time reached 73.10% after 120 min for Telon-blue, 59.57% after 40 min for Telon-orange and 50% after 60 min for Telon-red, while with increasing the temperature and adsorbent dose, adsorption capacity decreased. The highest adsorption using the composite PVP/Bt was obtained at pH = 6.15; adsorption capacity increased slightly as the stirring rate increased. Moreover, the pseudo-second-order model was more capable to describe the kinetic behavior of three Telon dyes adsorption in comparison with the pseudo-first-order model. The Freundlich isotherm model was more capable of describing the equilibrium behavior of the adsorption process than the Langmuir isotherm model. Furthermore, the thermodynamic parameters showed that the adsorption process was non spontaneous and exothermic.

ACKNOWLEDGMENTS

The authors thank the Laboratory of Catalysis and Synthesis in Organic Chemistry, University of Tlemcen, for XRD and TGA analysis.

REFERENCES

- [1] Anirudhan, T. S.; Suchithra, P. S., Humic acid-immobilized polymer/bentonite composite as an adsorbent for the removal of copper(II) ions from aqueous solutions and electroplating industry wastewater. *J. Ind. Eng. Chem.* **2010**, *16*, 130-139, DOI: org/10.1016/j.jiec.2010.01.006.
- [2] Adeymo, A. A.; Adeoye, I. O.; Bello, O. S., Adsorption of dyes using different types of clay. *Appl. Water Sci.* **2017**, *7*, 543-568, DOI: org/10.1007/s13201-015-0322-y.
- [3] Seow, T. W.; Lim, C. K., Removal of dye by adsorption: A review. *Inter. Appl. Eng. Res.* **2016**, *11*, 2675-2679.
- [4] Ozcan, A. S.; Erdem, B.; Ozcan, A., Adsorption of acid blue 193 from aqueous solutions onto BTMA-bentonite. *Colloids Surf. A, Physicochem. Eng. Asp.* **2005**, *266*, 73-81, DOI: 10.1016/j.colsurfa.2005.06.001.
- [5] Singh, K. P.; Mohan, D.; Sinha, S.; Tondon, G. S.; Gosh, D., Color removal from wastewater using low-cost activated carbon derived from agricultural waste material. *Ind. Eng. Chem. Res.* **2003**, *42*, 1965-1976, DOI: 10.1021/ie020800d.
- [6] Zen, S.; El Berrichi, F. Z., Adsorption of tannery anionic dyes by modified kaolin from aqueous solution. *Desalin. Water. Treat.* **2014**, *57*, 6024-6032, DOI: 10.1080/19443994.2014.981218.
- [7] Chai, K.; Ji, H., Dual functional adsorption of benzoic acid from wastewater by biological based chitosan grafted β -CD. *Chem. Eng. J.* **2012**, *203*, 309-318, DOI: 10.1016/j.cej.2012.07.050.
- [8] Liu, P., Polymer modified clay minerals: A review. *Appl. Clay. Sci.* **2007**, *38*, 64-76, DOI: 10.1016/j.clay.2007.01.004.
- [9] Pavlidouna, S.; Papaspyrides, C. D., A review on polymer layered silicate nanocomposites. *Prog. Polym. Sci.* **2008**, *33*, 1119-1198, DOI: 10.1016/j.progpolymsci.2008.07.008.
- [10] Nguyen, Q. T.; Baird, D. G., Preparation of polymer-clay nanocomposites and their properties. *Adv in Polym Tech.* **2007**, *25*, 270-285, DOI: org/10.1002/adv.20079.
- [11] Baybas, D.; Ulusoy, U., Adsorptive features of polyacrylamide aluminosilicate composites for methylene blue. *Turkish. Chem.* **2016**, *40*, 147-162, DOI: 10.3906/kim-1504-32.
- [12] Suteu, D.; Biliuta, G.; Rusu, L.; Coseri, S.; Nacu, G., Cellulose cellets as new type of adsorbent for the removal of dyes from aqueous media. *Envir. Eng. Manag. J.* **2015**, *14*, 525-532, DOI: 10.30638/eemj.2015.056.
- [13] Aboufazeli, F.; Reza Lotfi Zadeh Zhad, H.; Sadeghi, O.; Karimi, M.; Najafi, E., Synthesis and characterization of novel polythiophene-nanoporous silica and its application for mercury removal from waste waters. *J. Macromol. Sci., Part A: Pure Appl. Chem.* **2013**, *50*, 18-24, DOI: org/10.1080/10601325.2013.735955.

- [14] Karabörk, M.; Gök, A., A novel ion-imprinted nanocomposite for selective separation of Pb²⁺ ions. *J. Macromol. Sci., Part A: Pure Appl. Chem.* **2018**, *55*, 90-97, DOI: org/10.1080/10601325.2017.1387494.
- [15] Gadiri, A.; Benkhaled, A.; Choukchou-Braham, E., Equilibrium, kinetic and thermodynamic studies of copper adsorption onto poly (n-vinylpyrrolidone) modified clay. *J. Macromol. Sci., Part A: Pure Appl. Chem.* **2018**, *55*, 393-400, DOI: 10.1080/10601325.2018.1453258.
- [16] Anirudhan, T. S.; Suchithra, P. S.; Radhakrishnan, P. G., Synthesis and characterization of humic acid immobilized-polymer/bentonite composites and their ability to adsorb basic dyes from aqueous solutions. *Appl. Clay. Sci.* **2009**, *43*, 336-342, DOI: 10.1016/j.clay.2008.09.015.
- [17] Wan Ngah, W. S.; Md Ariff, N. F.; Hashim, A.; Megat Hanafiah, M. A. K., Malachite green adsorption onto chitosan coated bentonite beads: isotherms, kinetics and mechanism. *Clean-Soil. Air. Water.* **2010**, *38*, 394-400, DOI: org/10.1002/clen.200900251.
- [18] Yildiz, G.; Filiz Senkal, B., Formation of composites between polyvinylimidazole and bentonites and their use for removal of remazol black B from water. *Sep. Sci. Tech.* **2016**, *51*, 2596-2603, DOI: org/10.1080/01496395.2016.1165707.
- [19] Séquaris, J. M.; Hild, A.; Narres, H. D.; Schwuger, M. J., Polyvinylpyrrolidone adsorption on Na-montmorillonite. Effect of the polymer interfacial conformation on the colloidal behavior and binding of chemicals. *J. Colloid Interf. Sci.* **2000**, *230*, 73-83, DOI: org/10.1006/jcis.2000.7046.
- [20] Habiby, S. R.; Esmaili, H.; Foroutan, R., Magnetically modified MgO nanoparticles as an efficient adsorbent for phosphate ions removal from wastewater. *Sep. Sci. Technol.* **2019**, *40*, 1-12, DOI: 10.1080/01496395.2019.1617744.
- [21] Zhirong, L.; Azhar Uddin, Md.; Zhanxue, S., FT-IR and XRD analysis of natural Na-bentonite and Cu(II)-loaded Na-bentonite. *Spectrochimica. Acta. Part A.* **2011**, *79*, 1013-1016, DOI: 10.1016/j.saa.2011.04.013.
- [22] Zidan, H. M.; Abdelrazek, E. M.; Abdelghany, A. M.; Tarabiah, A. E., Characterization and some physical studies of PVA/PVP filled with MWCNTs. *J. Mater. Res. Technol.* **2018**, *8*, 904-913, DOI: org/10.1016/j.jmrt.2018.04.023.
- [23] Israel, L.; Zipkin, H.; Guler, C., Adsorption of poly (Vinylpyrrolidone) on sodium, calcium and aluminium montmorillonite. *Colloids and Surf. A: Physicochem. Eng. Asp.* **2008**, *316*, 70-77, DOI:10.1016/j.colsurfa.2007.08.025.
- [24] Piscitelli, F.; Posocco, P.; Toth, R.; Fermeglia, M.; Pricl, S.; Mensitieri, G.; Lavorgn, M., Sodium montmorillonite silylation: Unexpected effect of the aminosilane chain length. *J. Colloid. Interf. Sci.* **2010**, *351*, 108-115, DOI: 10.1016/j.jcis.2010.07.059.
- [25] Makhoukhi, B.; Villemin, D.; Didi, M. A., Synthesis of bisimidazolium-ionic liquids: Characterization, thermal stability and application to bentonite intercalation. *J. Taibah. Univ. Sci.* **2016**, *10*, 168-180, DOI: org/10.1016/j.jtusci.2015.08.005.
- [26] Makhoukhi, B.; Villemin, D.; Didi, M. A., Preparation, characterization and thermal stability of bentonite modified with bis-Imidazolium salts. *Mater. Chem. Phys.* **2013**, *138*, 199-203, DOI: org/10.1016/j.matchemphys.2012.11.044.
- [27] Mahini, R.; Esmaili, H.; Foroutan, R., Adsorption of methyl violet from aqueous solution using brown algae *Padina sanctae-crucis*. *Turk. J. Biochem.* **2018**, *43*, 1-9. DOI: 10.1515/tjb-2017-0333.
- [28] Marrakchi, F.; Bouaziz, M.; Hameed, B. H., Activated carbon-clay composite as an effective adsorbent from the spent bleaching sorbent of olive pomace Oil: process optimization and adsorption of acid blue 29 and methylene blue. *Chem. Eng. Res. Design.* **2017**, *128*, 221-230, DOI: 10.1016/j.cherd.2017.10.015.
- [29] Makhoukhi, B.; Didi, M. A.; Moulessehou, H.; Azzouz, A.; Villemin, D., Diphosphonium ion-exchanged montmorillonite for telon dye removal from aqueous media. *Appl. Clay. Sci.* **2010**, *50*, 354-361, DOI: 10.1016/j.clay.2010.08.026.
- [30] Choukchou-Braham, E.; Benabadi, K. I.; Benkhaled, A.; Sekkal, A. R.; Heddi, D.; Djamaa, Z., N-Octyl quaternized P4VP interaction with orange telon. *J. Macromol. Sci., Part A: Pure Appl. Chem.* **2015**, *52*, 273-279, DOI: org/10.1080/10601325.2015.1007272.

- [31] Esmaeili, H.; Foroutan, R., Adsorptive behavior of methylene blue onto sawdust of sour lemon, date palm, and eucalyptus as agricultural wastes. *J. Disper. Sci. Technol.* **2018**, 1-10, DOI: 10.1080/01932691.2018.1489828.
- [32] Abshirini, Y.; Foroutan, R.; Esmaeili, H., Cr(VI) removal from aqueous solution using activated carbon prepared from *Ziziphus spina-christi* leaf. *Mater. Res. Express.* **2019**, 6, 1-37, DOI: org/10.1088/2053-1591/aafb45.
- [33] Grelluk, M.; Hubicki, Z., Isotherm and thermodynamic studies of reactive black 5 removal by acid acrylic resins. *Chem. Eng. J.* **2010**, 162, 919-926, DOI: 10.1016/j.cej.2010.06.043.
- [34] Makhoukhi, B.; Djab, M.; Didi, M. A., Adsorption of telon dyes onto bis-imidazolium modified bentonite in aqueous solutions. *J. Envir. Chem. Eng.* **2015**, 3, 1384-1392, DOI: org/10.1016/j.jece.2014.12.012.
- [35] Ahmadi, F.; Esmaeili, H., Chemically modified bentonite/Fe₃O₄ nanocomposite for Pb(II), Cd(II), and Ni(II) removal from synthetic wastewater. *Desalin. Water. Treat.* **2018**, 110, 154-167, DOI: 10.5004/dwt.2018.22228.
- [36] Tamjidi, S.; Esmaeili, H., Chemically modified CaO/Fe₃O₄ nanocomposite by sodium dodecyl Sulfate for Cr(III) removal from water. *Chem. Eng. Technol.* **2019**, 42, 607-616, DOI: org/10.1002/ceat.201800488.
- [37] Khoo, F. S.; Esmaeili, H., Synthesis of CaO/Fe₃O₄ magnetic composite for the removal of Pb(II) and Co(II) from synthetic wastewater. *J. Serb. Chem. Soc.* **2018**, 83, 237-249. DOI: 10.2298/JSC170704098S.
- [38] Teimouri, A.; Esmaeili, H.; Foroutan, R.; Ramavandi, B., Adsorptive performance of calcined cardita bicolor for attenuating Hg(II) and as(III) from synthetic and real wastewaters. *Korean J. Chem. Eng.* **2018**, 35, 479-488. DOI: 10.1007/s11814-017-0311-y.